Functionalized Droplet Microfluidics: From Patterning to Sensing and Energy Harvesting

A thesis submitted
in partial fulfillment of the requirements
for the degree of

Doctor of Philosophy

by

Siddharth Thakur

Roll No. 156107004

Department of Chemical Engineering

Indian Institute of Technology Guwahati

November 2021

SYNOPSIS

Chapter I. Introduction

Mesoscopic liquid droplets are ubiquitous in nature. From sessile droplet-based diagnostic devices to rainwater energy harvesting - liquid droplets offer a versatile platform for the construction of functional systems. This unique geometry has been adapted across diverse scientific and engineering domains owing to its attractive characteristics. These characteristics have also aided in highlighting its potential to replace conventional processes at the macroscale. Some of the distinct advantages associated with liquid droplet systems at the micro/nanoscale includes: (i) limited usage of fluid volume with the smallest possible area available per unit mass, (ii) an incompressible system that is soft and deformable, (iii) thermodynamically an open system suitable for facile mass, momentum, and energy transfer through the surface, and (iv) facilitating the incorporation of different constituents that impart optically and electrochemically active properties.

Rapid progress in the field of science and technology has fostered the miniaturized devices that are more efficient than their macroscale counterparts. In this regard, the sessile droplet-based systems offer an attractive and alternate system configuration that can integrate and function on a large-scale to tackle numerous challenges. Since droplets- based systems have a high surface area to volume ratio, they are particularly prone to enhanced rates of mass and energy transfer with their surroundings. The confined system possessed by the droplet geometry allows uniform interaction with its surrounding environment via its curved interface, which lacks spatial inhomogeneities. Thus, in the presence of external fields, diffusion-limited processes such as chemical reactions, are facilitated owing to the formation of the convective flow patterns within a droplet, as characterized by a relatively high Reynolds number. For example, prior-art suggest the usages of thermal and solutal field gradients, for devising systems that can perform analyte sensing as well as energy harvesting.

Recent years have also witnessed the tremendous growth of hybrid systems in the healthcare sector. These alternate methodologies have employed facile and effective detection strategies for confronting the major issue of affordable diagnostic devices for low-resource settings. In this regard, microfluidic technologies have presented a promising route for facilitating storage, reaction, and separation of identifying biomarkers. For instance, liquid droplet systems have carried out rapid analysis either by utilizing evaporative-based techniques or operating in the presence of other field-driven methodologies. Moreover, given the versatile nature of droplets-based systems, in particular water droplet-based platforms, it is not surprising that of late an increasing number of studies have focused on its usage for addressing another critical issue of harvesting ambient energy. For example, the triboelectric generators have exploited the polar nature of the water microdroplets for harvesting energy from the electrical-double layers formed near the surfaces where the droplets impinge. Other measures such as microscale fuel cells involve the addition of reactive components that can enhance the conversion of chemical to electrical energy. The advantage lies with their ability to incorporate elements such as photosensitive electrodes while connecting serially on a large-scale to generate high-density power. Such a range of adaptations has only aided in the deployment of droplet-based platforms for tackling futuristic issues.

On the other hand, different facets of liquid droplets offer opportunities for utilization towards different objectives. Physical characteristics such as the droplet curvature have been utilized for magnification purposes in optics-related tasks. In this aspect, modification of the droplet medium from isotropic to anisotropic have been reported to provide an additional handle over light-manipulation capabilities. For macroscale applications, it becomes vital to assimilate a multitude of such uniform optically-active structures that can be employed as fluidic lenses or photomasks. As compared to the expensive photo/electron lithographic-based techniques, dewetting processes involving fluids or soft-lithographic techniques offer an affordable route towards the realization of these structures. Furthermore, with regards to optics-related applications, functional materials such as the ionic liquids or liquid crystals (LC) have been increasingly investigated. The internal molecular ordering of LC can be tailored using various external stimuli such that the output light is transmitted accordingly. Exploring LC thin film dewetting processes on soft, slippery surfaces may present a facile way for creating numerous self-organized micro/nano-droplets for photonic applications.

Considering such characteristics of droplet platforms, it becomes abundantly clear that their role is expanding across different domains at the micro/nanoscale, leading to the generation of alternate technological solutions. In this dissertation, different field-driven systems including acoustic, photonic and chemical-potential, have been selectively utilized for exploring the underlying physics associated with droplet platforms towards patterning, sensing and energy harvesting applications. Micro-scale experimental setups employing solid and liquid substrates have been utilized to uncover the different phenomenon associated with such droplet systems. The point-wise objectives concerning the different chapters in this thesis are as follows:

- Investigation of acoustic wave catalyzed urea detection employing a pulsatile sonophillic microdroplet sensor.
- Exploring microdroplet photofuel cells for harvesting high-density energy capable of simultaneously working as a dye degradation platform.
- Generation of self-organized liquid crystal microdroplets for utilization as tunable soft-photomasks.
- Chemotactic dewetting of a nematic liquid crystal droplet on a liquid bath.

In the subsequent sections II–V of this report, primary details highlighting the different technical aspects belonging to the thesis chapters have been provided. A short summary of the various works along with the scope for future research in these areas has also been provided.

Chapter II. Acoustic Wave Catalyzed Urea Detection Utilizing a Pulsatile Microdroplet Sensor

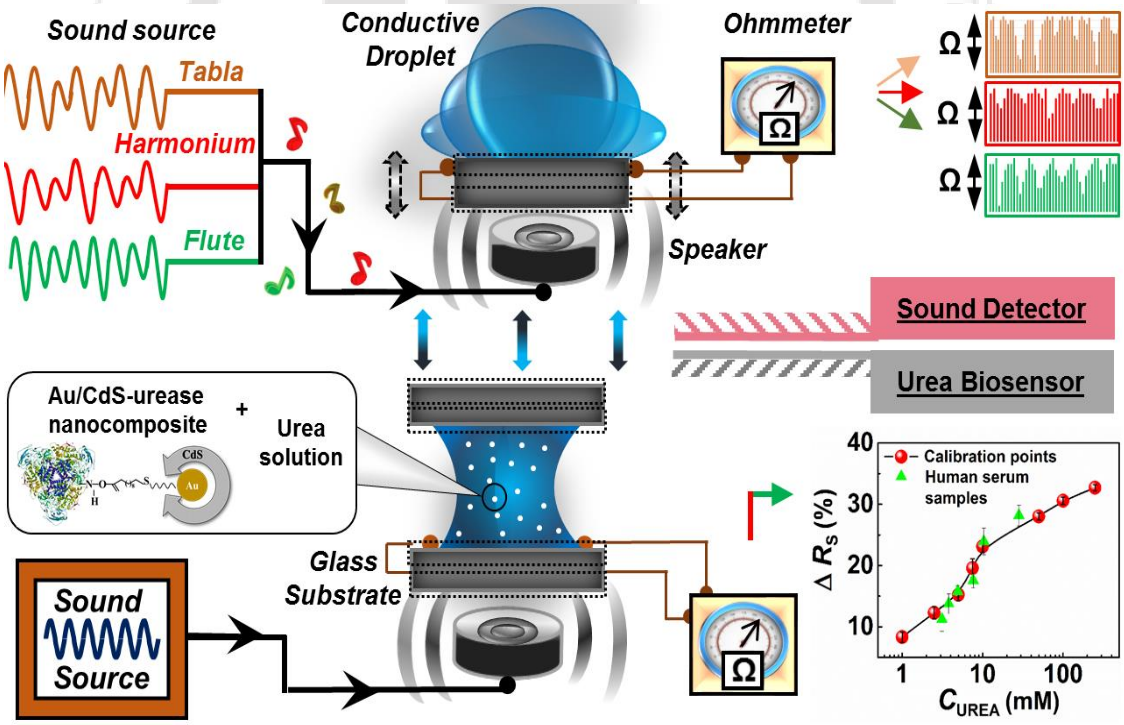

Figure 1. Overall schematic of droplet-based sensor. A freestanding configuration was used to sense the changes in acoustic signals emanating from different instruments. Further, a sandwich configuration was utilized to sense the urea concentrations within an unknown serum sample.

In this chapter, we observe and utilize the variations measured in the electrical resistance across a conducting water microdroplet when it is placed on a glass substrate and mechanically vibrated at the natural frequency of the setup with the help of an acoustic source. The reduction in the resistance across the droplet was magnified owing to the formation of vortices in the matrix when the periodic oscillation of the substrate was increased. The variation in the resistance could be tuned with the frequency of the sound source, which was found to be maximum when a 10 μL droplet was vibrated at ~320 Hz. Interestingly, the variation in resistance across the oscillating droplet could follow and distinguish the musical notes in the octaves – “sur”, or rhythmic cycles – “taal”, originating from the Indian-origin musical instruments such as, flute, harmonium, whistle, and tabla.

Further, when a suspension of urease-stabilized gold-cadmium-sulfide nanocomposite was suspended inside the droplet, and mixed with an analyte containing urea solution, the change in the resistance during the operational time period was found to monotonically vary with the concentration of urea in the analyte. The enzymatic reaction between urea and urease was found to follow a faster first-order chemical kinetics than the commonly observed Michaelis–Menten pathway owing to the presence of the moving nanocomposites and mixing-vortices under the optimal acoustic excitations. The specific lock-and-key enzymatic reaction helped in extending these experimental results to estimate the unknown levels of urea in human blood serum samples.

Chapter III. Microdroplet PhotoFuel Cells to Harvest High Density Energy and Dye Degradation

This chapter presents the design and development of a membraneless photofuel cell, namely μ-DropFC, to harvest chemical and solar energies simultaneously. The droplet prototype also performed environmental remediation to demonstrate its multitasking potential as a sustainable hybrid device in a single embodiment. Hydrogen peroxide (H_2O_2) microdroplet at optimal pH and salt loading was utilized as the fuel, integrated with an Al anode and zinc phthalocyanine coated Cu cathode. The presence of n-type semiconductor zinc phthalocyanine in between the electrolyte and metal enabled the formation of a photo-active Schottky junction suitable for power generation under light. Concurrently, the oxidation and reduction of H_2O_2 on the electrodes helped in the conversion of chemical energy into the electrical one in the same membraneless setup. Suspension of Au nanoparticles (NPs) in the droplet helped in enhancing the overall power density under photonic illumination through the effects of localized surface Plasmon resonance (LSPR). Further, the presence of photo-active n-type CdS NPs enabled catalytic photo-degradation of dyes under light in the same embodiment.

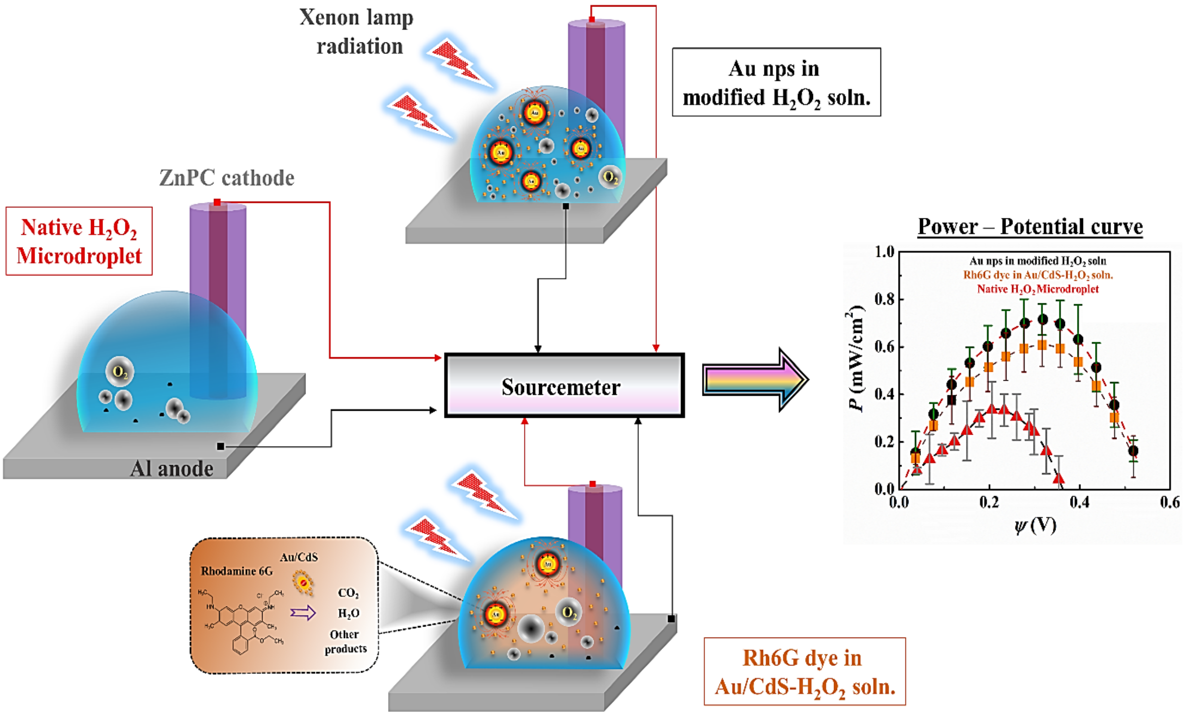

Figure 2. Overview of the hybrid membraneless droplet-based photofuel cell (μ-DropFC). Utilization of Au NPs in a H2O2 μ-DropFC enhanced the overall power density in presence of external radiations. Interestingly, the same droplet configuration could also harvest significant energy while being engaged in degradation of an environmental pollutant.

A 40 μL μ-DropFC could show a significantly high open circuit potential of ~0.58 V along with a power density of 0.72 mW/cm^2. Under the same condition, integration of ten such μ-DropFCs produced a power density of ~7 mW/cm^2 at an efficiency of 3.4%. Moreover, the μ-DropFC also degraded ~85% of an industrial pollutant Rhodamine 6G in 1 h while generating a power density of ~ 0.6 mW/cm^2. The performance parameters of μ-DropFC were found to be either comparable or superior to the existing prototypes. In a way, the membraneless and high-performance μ-DropFC harnessed energy from multiple sources while engaging in environmental remediation.

Chapter IV. Self-Organized Liquid Crystal Droplets as Tunable Soft-Photomasks

Utilization of liquid/liquid dewetting methodology for the generation of large-area, miniaturized, distinct, and stable droplets offer itself as a promising scalable technique for catering to a wide variety of micro/nano applications. In this chapter, a single-step pathway was presented to generate a multitude of quasi-monodispersed LC droplets obtained via the spreading of a 4-Cyano-4'-pentylbiphenyl (5CB)-laden hexane droplet over a CTAB-water bath. A facile soft-photolithography setup was prepared to incorporate these 5CB droplets as fluidic photomasks for the generation of distinct features over photoresist (PR) surfaces.

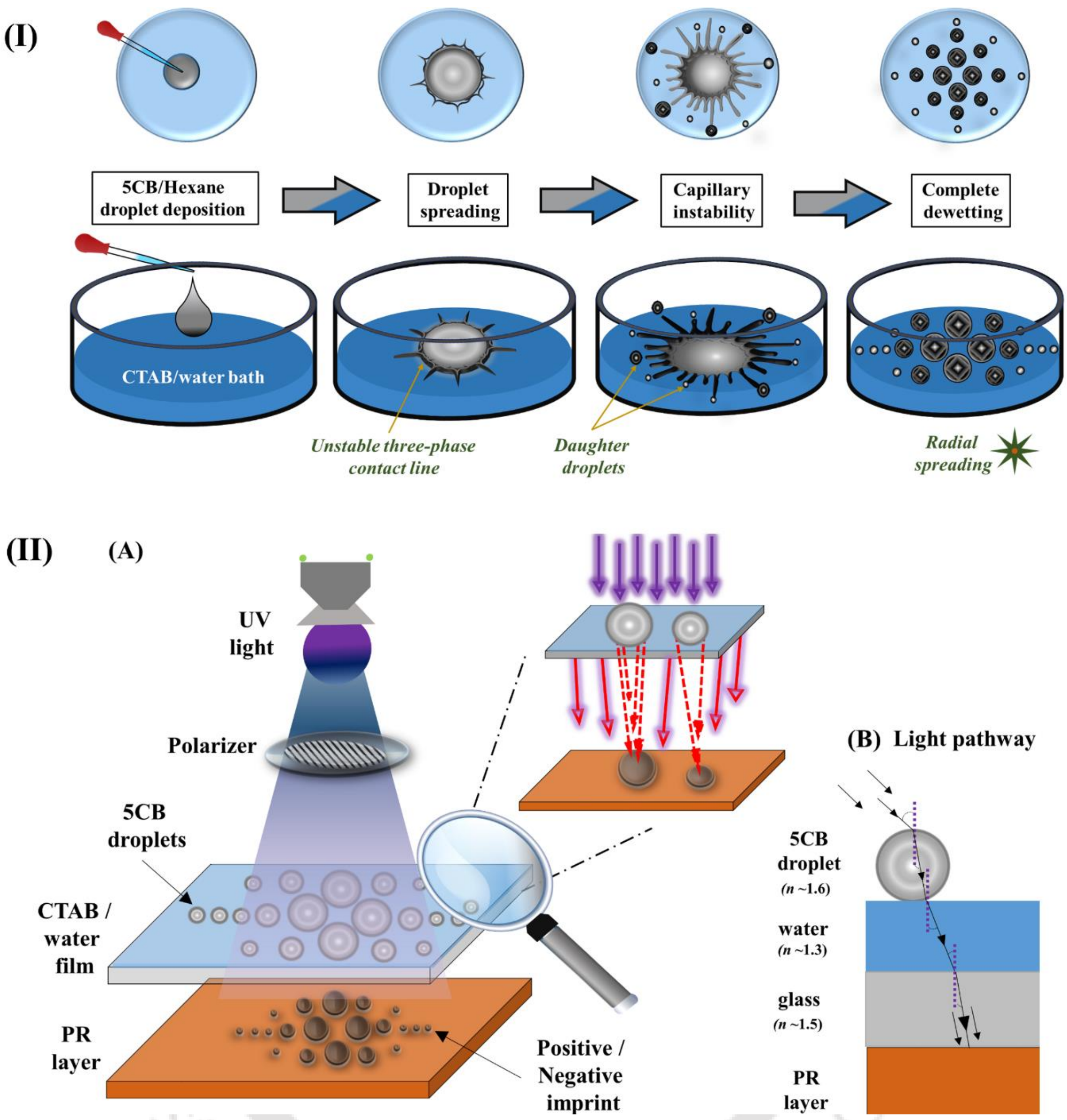

Figure 3. Schematic diagram highlighting the phenomenon and application of dewetting of the liquid bilayer. (I) A 5CB-hexane compound droplet was dispensed over a CTAB-laden water bath. Rapid spreading and subsequent retraction of the compound droplet led to generation of multitude of 5CB droplets from the contact line. (II) (A) 5CB droplets were used in a soft-photolithography setup for obtaining unique patterns on a photoresist (PR) substrate. (B) Light path from the surroundings to the PR surface. *n* represents the refractive index of material.

For two different PR tones, surface features with micron to nano-scale dimensions were obtained over a large area: flattened droplets were obtained on a positive photoresist substrate while donut-like features were obtained on a negative photoresist substrate. Solvent vapor annealing of the LC droplets led to their phase transition, which provided an additional handle over the diversity of patterns obtained. The dewetting dynamics concerning 5CB droplet dewetting was greatly influenced by the surface-active agent (CTAB) concentration. Low concentrations favored laminar spreading of the droplet with gradual retraction, while at high concentrations (beyond critical concentration limit), droplet dynamics was difficult to follow due to rapid and uneven retraction profiles on account of a heterogeneous surface-energy substrate. The solvent selection also played a role in governing the overall dewetting period along with the dimensions of daughter droplets generated over the water-surfactant bath: hexane promoted a fast-dewetting phase with miniaturized droplets generation (1–90 μm) while heptanol resulted in slow dewetting dynamics with irregular, large daughter droplets (> 100 μm). Different dewetting modes for 5CB were observed across two other solvents viz. toluene and chloroform. Remarkably, the dewetting dynamics displayed by 5CB was not material-specific and was observed in polystyrene-toluene solution over the water-surfactant bath.

Chapter V. Chemotactic Dewetting of a Nematic Droplet on a Water Bath

Techniques involving the creation of miniaturized optically-active droplets without the need for cumbersome instrumentation highlight their potential for being adapted towards large-scale operations. In this chapter, experimental investigations uncover the dynamics associated with a nematic LC droplet when it is placed on an immiscible liquid bath, in the vicinity of a miscible solvent droplet. A 5CB droplet on a water bath displays various contact line dynamics when a hexane droplet is dispensed close to it. The highly volatile hexane interacts with the 5CB droplet during its adsorption on 5CB surface as well as during spreading on the water bath. In both case, this results in the lowering of local surface tension gradient within the 5CB droplet. This surface tension gradient across the droplet bulk led to the initiation of recirculation within the 5CB droplet matrix. An osmotic pressure gradient was also created on the water interface, which along with the convective forces within the water bath, aided in the 5CB droplet motility. Beyond a critical recirculation rate within the 5CB droplet, centripetal forces generated due to the recirculation overcome the surface tension forces resulting in the instantaneous distortion of the droplet boundary. It was observed that the recirculation ceases to exist at the point of distortion, and gradually picked-up over a period of time, with the process repeating itself. Furthermore, at the 5CB droplet boundary facing hexane, the spreading of the 5CB droplet on the water bath led to the creation of numerous 5CB droplets which resisted coalescence. The spreading of the droplet was followed by the occurrence of capillary instability at the droplet periphery.

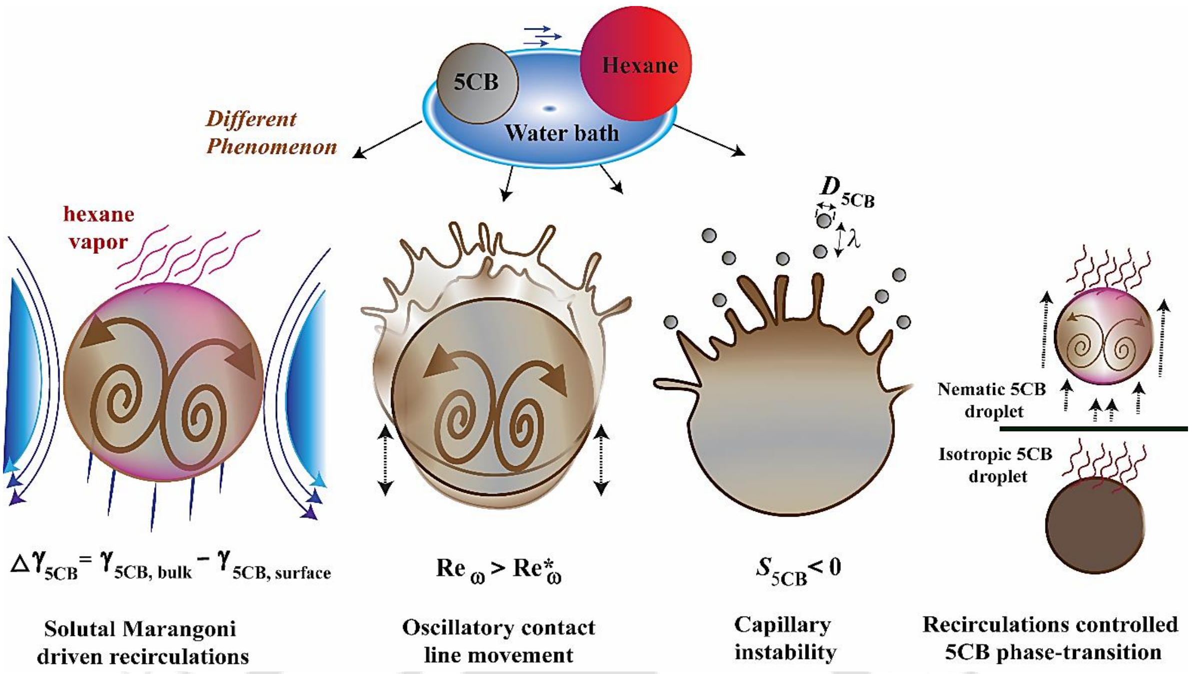

Figure 4. Overview of the entire process. Isolated 5CB and hexane droplets when placed at a close distance on a water bath display numerous spatiotemporal droplet dynamics. Initially, the solutal Marangoni effect initiates recirculation within the 5CB droplet owing to the surface tension gradient between the surface and bulk 5CB. This recirculation initiates convective flow within the water bath that aids in the droplet motility. Beyond a certain recirculation rate, centripetal forces generated within the droplet overcome surface tension at the periphery that results in periodic oscillations of the 5CB droplet. Moreover, the droplet region close to the hexane source undergoes spreading on the water bath. The thin film eventually undergoes capillary instability as the hexane evaporates and changes the local spreading coefficient. Remarkably, the recirculation set in within the droplet enhance the rate of adsorption of hexane which causes the phase transition of 5CB from nematic to isotropic. Once in the isotropic phase, the droplet no longer displays any lateral or longitudinal movement on the water bath.

Additionally, in presence of hexane, the recirculation was also observed to enhance the rate of phase transition in the 5CB droplet from nematic to isotropic as it led to faster uptake of hexane. Once in the isotropic state, the droplet resisted further oscillation or lateral/longitudinal movement because of the reduction in the surface tension gradient.

Chapter VI. Conclusions and Future Scope

This thesis presents various proof-of-concept droplet systems highlighting their versatility and applicability towards applications ranging from biosensing and energy harvesting to patterning. The second chapter highlights the utility of a facile setup that employs an acoustically vibrated conducting water microdroplet tailored for sensing purpose. It was observed that the vibrations imparted to the microdroplet resulted in the variation of electrical resistance across it, which was measured by the two electrodes placed at diametrically opposite ends of the droplet. The change in the electrical resistance of the droplet could be correlated with the change in external acoustic signal. Variation in the external signal frequency and tempo could be distinguished thereby facilitating the droplet setup to be used as a sound sensor. Additionally, the similar detection principle was also employed for the development of a urea biosensor. Doping the droplet with Au/CdS nanocomposite linked urease enzyme and stimulating it with acoustic signals in presence of urea solution, led to the preparation of a calibration curve. Herein, the change in urea concentration within the droplet could be correlated to the change in electrical resistance across the droplet. It was also observed that the rate of urea-urease enzymatic reaction was significantly faster in presence of acoustic signals. Better interaction between constituents was due to presence of recirculation as a result of the vibrating substrate, and presence of Au/CdS nanocomposite which offered a higher interfacial area for the reaction. Comparison of the microdroplet-based urea biosensor with a standard laboratory technique revealed that the droplet sensor could determine unknown urea levels in serum samples within a 10% - 15% margin of error.

The third chapter explores the role of a microdroplet as a hybrid energy harvesting setup. The droplet utilized hydrogen peroxide as the fuel and oxidant, and ZnPC/Cu, and Al as cathode and anode, respectively. Electrochemical energy harvesting could be achieved as the droplet operated as a photofuel cell system. Presence of additives such as Au NPs aided in enhancing the power and current density values. In presence of external illumination, the LSPR effect of the Au NPs increased the localized electric field intensity which improved the charge transfer characteristics between electrodes and suppressed charge recombination at the ZnPC electrode. A 40 µL µ-DropFC could generate an open circuit potential of ~0.58 V and power density of 0.72 mW/cm^2. Utilizing the same droplet composition in a VLSI configuration of 10 cells generated a power density of ~7 mW/cm^2 at an efficiency of 3.4%. It was also observed that the same droplet setup could be employed as a dye degradation unit. Rhodamine 6G dye was added to the droplet and within an hour ~ 85% of the dye was degraded. Moreover, energy harvesting during this operation resulted in generation of ~ 0.6 mW/cm^2, thereby highlighting the hybrid characteristic of the setup of that being able to generate energy while being engaged in dye degradation.

The fourth chapter discusses a pathway to realize self-organized optically-active 5CB droplets on a large-scale that was employed as photomasks in a photolithography experiment. Experiments involving the deposition of a 5CB-in-hexane drop on a CTAB laden water bath were carried out. Rapid spreading of the 5CB-in-hexane droplet was assisted by the interfacial tension gradient. After reaching equilibrium, the leading edge of the drop was observed to retract at a gradually slow rate. Varying the CTAB concentration led to the emergence of two modes of dewetting – spinodal (below CMC limit) and heterogeneous (above CMC limit). The retraction of the 5CB compound droplet led to the ejection of numerous daughter 5CB droplets from the three-phase contact line due to capillary instability. The dimensions of the daughter 5CB droplets could be primarily controlled by varying the 5CB concentration and CTAB concentration. Furthermore, these miniaturized 5CB droplets were utilized as soft photomasks in an unconventional photolithography setup to generate diverse 2D, 3D patterns. Solvent vapor annealing provided an additional handle over light modulation and subsequent generation of features. Experiments also revealed that changing the 5CB solvent led to new modes of dewetting over the CTAB bath. Additionally, these dewetting routes were not 5CB specific and were observed in case of polystyrene-solvent drop deposition as well.

The fifth chapter investigates the striking contact line dynamics displayed by the pristine 5CB droplet when it is deposited on a water bath in presence of a hexane droplet. A facile route for generation of multitudes of miniaturized 5CB droplets was uncovered. Hexane adsorption on the 5CB droplet surface as well as its contact with the 5CB droplet over the water bath, results in change of local surface tension within the nematic droplet. The solutal Marangoni stresses generates a plurality of instabilities such as recirculation within the 5CB droplet bulk, and oscillatory contact line motion along with 5CB droplet ejection at the three-phase contact line. It was observed that the recirculation within the 5CB droplet increased gradually until reaching a critical value. Thereafter, the centripetal forces overcame the surface tension forces leading to an instantaneous distortion of contact line, leading to droplet spreading. This was immediately followed by cessation of the recirculation which also led to restoration of the circular 5CB droplet imprint and this entire cycle repeated thereafter. Osmotic pressure gradient near 5CB periphery also enforces a net change in the *S* value across the 5CB droplet such that droplet motility on the water bath is observed. Experiments uncover that variation in the water bath level controls the rate of droplet motility. Furthermore, volume of hexane droplet deposited on water bath also influenced the rate of 5CB recirculation. Increasing the bath temperature led to faster recirculation on the account of thermal Marangoni effects, however it reduced the recirculation time period as 5CB phase transition occurred early. Increasing the salt concentration of the water bath also enhanced the rate of recirculation significantly, which as a result, increased hexane uptake, reducing overall recirculation period.

The different droplet-based applications and phenomena presented in this dissertation highlights the immense potential of these miniaturized systems. It further introduces a number of avenues for potential future research. Designing of acoustic sensors employing audible sounds for droplet stimulation highlights a facile and affordable sensing methodology. Further improvement with respect to device efficiency can be brought out by analysing droplet-substrate interaction by incorporating patterned electrodes for contact line pinning and assessing ionization effects of electrode prior to analyte loading. Moreover, utilization of multiple enzyme-doped droplets for a multiplex assay can lead to a promising lab-on-a-chip point of care sensor. Microdroplet photofuel cells are an alternative energy harvesting system capable of fulfilling multi-functional objectives. As presented here, simultaneous dye degradation while generation of energy from the hydrogen peroxide based redox reaction, could be realized. Further research into areas such as fuel selection, anode stability and identification of low-onset potential cathode can significantly aid in enhancing the device parameters. Additionally, designing of better circuits for VLSI may lead to accomplishing stand-alone power sources for deployment in remote locations for low energy-intensive systems. Utilizing the different aspects of droplet-dynamics on various substrates can lead to emergence of alternate approaches for solving conventional issues.

Liquid-on-liquid dewetting phenomenon has been analysed incorporating LC, for obtaining multitudes of optically-active, miniaturized nematic droplets. These droplets have been utilized as soft photomasks in an unconventional photolithography setup for obtaining unique 2D, 3D patterns. This route of large-scale nematic droplet generation can be analysed for different LCs possessing smectic, cholesteric and other exotic LC phases, in order to get tailored photomasks generating diverse features on PR surfaces. Also, theoretical investigation of the spreading and retracting dynamics may lead to a better understanding of the governing forces and aid in controlling dimensions of daughter droplets. LC droplet interaction on an aqueous surface in presence of a solvent droplet has shown to display striking spreading dynamics. Different modes of instability have been visualized due to influence of solutal Marangoni effect. Moreover, this phenomenon also helps to obtain miniaturized LC droplets, with a 10^5 order of magnitude reduction. In-depth analysis into the various contact line instabilities near the LC droplet can lead to better understanding of the dewetting phenomenon. This may help explore the contact phase dynamics of miscible and immiscible systems on soft, deformable substrates. Furthermore, this technique can also be harnessed for generation of compound LC droplets utilized in biosensing, material synthesis and photonics applications.